Section A-Research paper

Possible Role of Magnetic Resonance Imaging in Adnexal Masses

Mohamad Mohamad Al-Bakry[1], Ahmed Mohamed El-Hosseiny[1], Osama Abdallah Dawood[2], Khaled Fathy Helal[1], Ahmed Hisham Saleh Radwan[1]

1 Obstetrics and Gynecology Department, Faculty of Medicine, Zagazig University, Egypt
2 Diagnostic Radiology Department, Faculty of Medicine, Zagazig University, Egypt
Email: Drahmedheshamsaleh@gmail.com, AHsaleh@medicine.zu.edu.eg, ahmedhesham2023gm@gmail.com

Article History: Received 10th June, Accepted 5th July, published online 10th July 2023

Abstract

Background: Ovarian cancer is the second most common gynecologic malignancy in resource-rich countries and the third most common gynecologic malignancy in resource-limited countries (cervical cancer is the most common). Management of women with adnexal masses is frequently guided by imaging findings; therefore, precise characterization of adnexal pathology should be performed whenever possible. Magnetic resonance imaging is useful in characterization of adnexal masses that are not completely evaluated by ultrasound because it can provide additional information on soft tissue composition of adnexal masses based on specific tissue relaxation times and allows multiplanar imaging at large field of view to define the origin and extent of pelvic pathology.

Keywords: Magnetic Resonance Imaging, Adnexal Masses

Introduction

Management of women with adnexal masses is frequently guided by imaging findings; therefore, precise characterization of adnexal pathology should be performed whenever possible. Magnetic resonance imaging is useful in characterization of adnexal masses that are not completely evaluated by ultrasound because it can provide additional information on soft tissue composition of adnexal masses based on specific tissue relaxation times and allows multiplanar imaging at large field of view to define the origin and extent of pelvic pathology **(1).**

Magnetic resonance imaging was shown to be the most appropriate investigation for patients with an indeterminate adnexal mass on ultrasound, i.e. pelvic lesions in which either the organ of origin is uncertain or it remains unclear whether the nature is benign or malignant **(1).**

Ovaries show low to intermediate signal intensity like the myometrium on T1 weighted sequences and may be hard to separate from adjacent uterus or bowel. The ovaries can usually be easily identified on T2 weighted sequences due to the characteristic presence of clustered small high signal intensity follicles or cysts in the stroma of intermediate signal intensity. The ovaries may be difficult to be identified in the premenarchal and postmenopausal patient, due to the absence of follicles. Fat saturation may be employed to increase visualization of the ovaries in this situation **(2).**

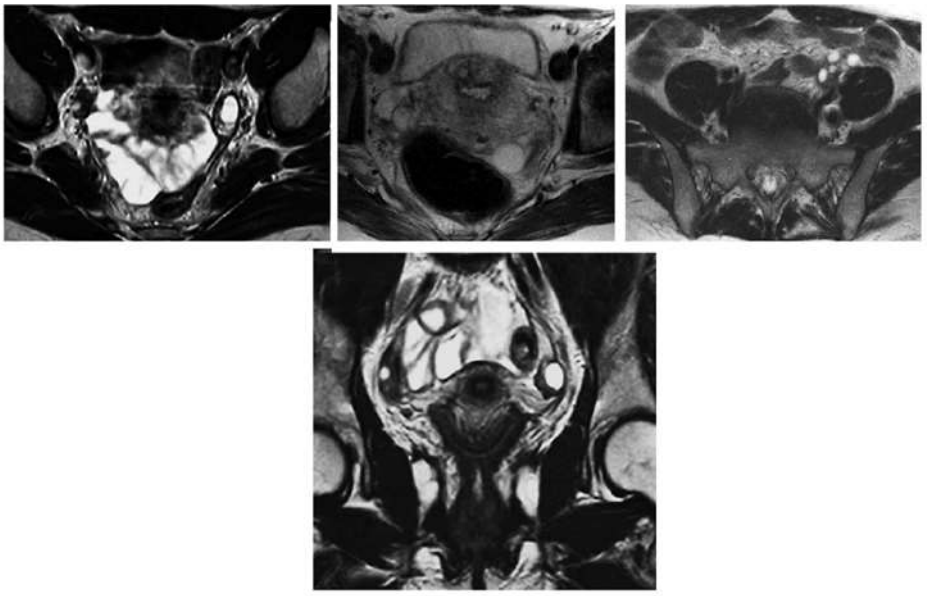

Fig.1: Gynecologic MRI, multiple sequences, showing normal ovar***y*** **(2).**

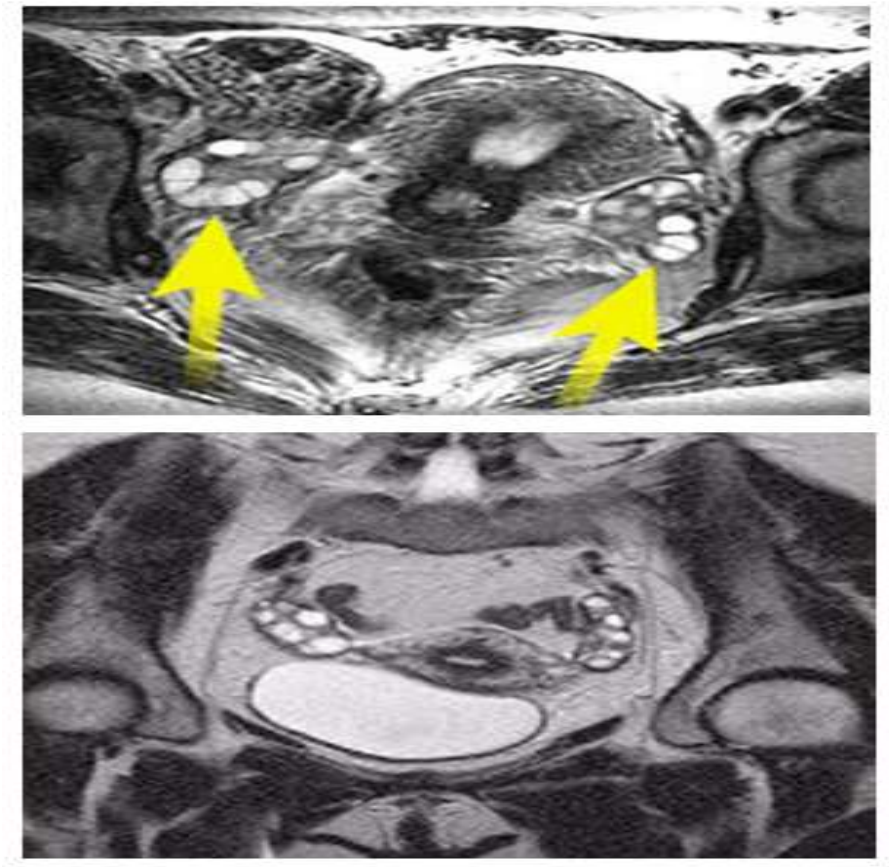

Fig. 2: Gynecologic MRI. (a) Axial T2WI of the female pelvis, the ovaries (arrows) are depicted clearly because of the fluid within the follicles and (b) high resolution T2WI, coronal view showing clearly both ovaries **(3).**

MRI manifestations of ovarian tumors

The main role of using MRI in assessment of ovarian masses is its capability to characterize tissues. The presence of hemorrhage, fat, mucin, fluid, and solid components in an ovarian mass can be described with the help of MRI **(3).**MRI can be used in the evaluation and in pre-operative planning in cases of advanced ovarian cancer where pelvic spread is suspected or in cases of pelvic recurrence. It is the best method for detection of infiltration to the uterus, bladder, rectum or pelvic sidewall. MRI is indicated in patients who have allergy to iodinated contrast media, pregnant or in cases where the CT findings are inconclusive or negative **(3).**

The imaging criteria for malignant ovarian tumors by the MRI include:

The 1ry criteria include:

- A slid or large solid area within a cystic mass.
- Wall thickness more than 3 mm.
- Septal thickness more than 3 mm and/or vegetations or nodularity.
- Necrosis.

The ancillary criteria include:

- Infiltration of pelvic organs or the sidewall.
- Peritoneal, mesenteric, or omental disease.
- Ascites.
- Lymphadenopathy **(4).**

MRI findings of common ovarian masses:

- **Serous cystadenomas:** commonly appear as unilocular cyst with thin wall and contain clear fluid. So, on T1 WI it shows low signal intensity, and show high signal intensity on T2WI in uncomplicated cases **(4).**

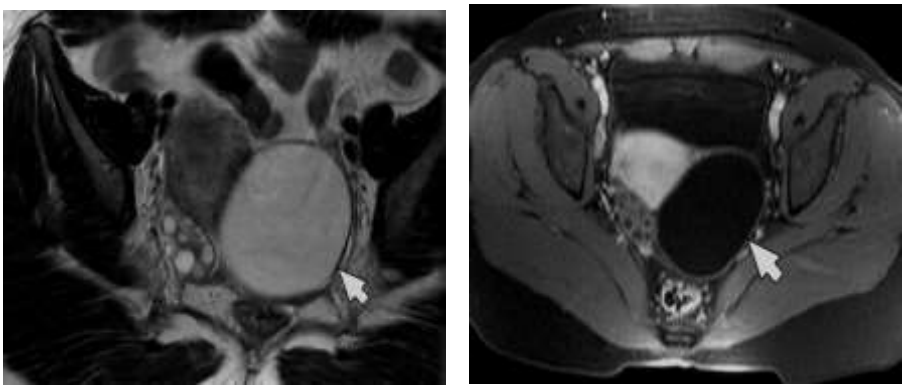

Fig.3: A 33-year-old woman with 8-cm serous cystadenoma of left ovary (a) axial unenhanced T2-weighted images showing hyperintense left ovarian cyst. (b)Gadolinium enhanced spoiled gradient-echo T1-weighted showing uniform enhancing wall with no enhancing solid parts **(4).**

- **Mucinous cystadenoma:** is bigger than serous tumors with multilocular cysts. They contain gelatinous material or fluid of various viscosities having on both T1W and T2W various signal intensities and so-called "stained glass" appearance**,** high signal intensity fluid on T1- and T2-WI indicates fresh hemorrhage (especially in serous cystadenoma) or mucin **(4).**

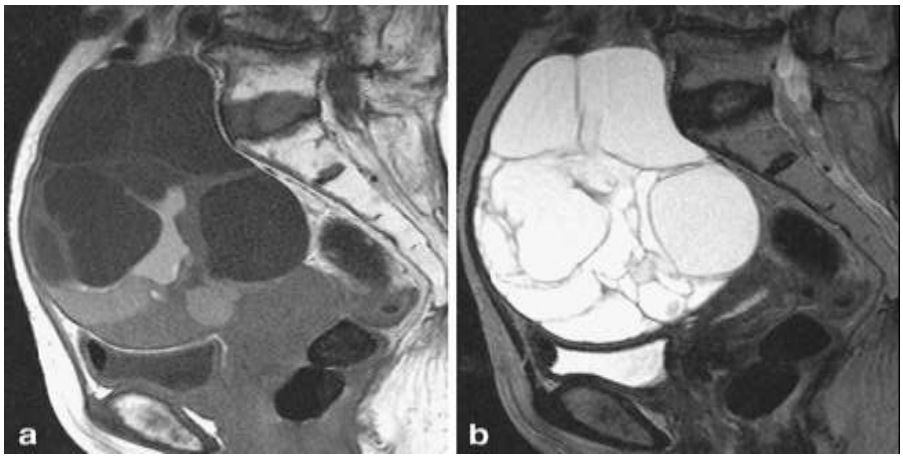

Fig. 4: Mucinous cystadenoma in an 83-year- old woman. (a) Sagittal T1 and(b) T2- weighted magnetic resonance (MR) images show a cystic lesion containing multiple locules of varying signal intensities presenting as a stained-glass appearance **(4).**

- **Borderline tumors:** can show extra papillary projections than can be infrequently seen in cystadenomas. Pathologic and MR imaging studies have suggested that large papillary projections with no solid component denote a borderline or malignant tumor **(5).**

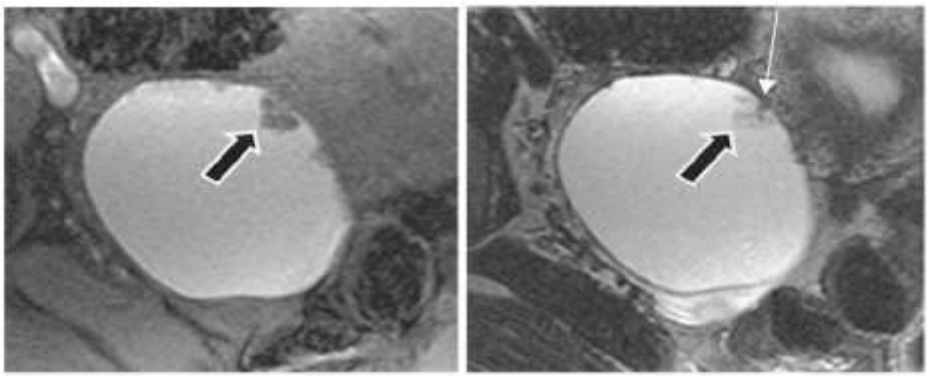

Fig. 5 : Borderline papillary serous tumor in a 48-year-old woman with an elevated serum CA-125 level (a) Fat-saturated T1-weighted gradient-echo MR image shows excrescences (arrow) as fronds that have lower signal intensity than the cyst fluid. (b) T2-WI shows papillary projections (thick arrow) with a low-signal-intensity core (thin arrow) **(6).**

Endometriod tumors: are frequently large, complex cystic mass with solid component. They are bilateral in 25 - 40% of cases. It may be associated with endometrial thickening or endometriosis or even associated endometrial carcinoma. Endometriod carcinoma would be considered when the MRI images show a cystic mass with irregular solid component associated with endometrial carcinoma, it shows a relatively low signal intensity of the tumor wall on T2 WI and .can show mild enhancement on T1 WI **(7).**

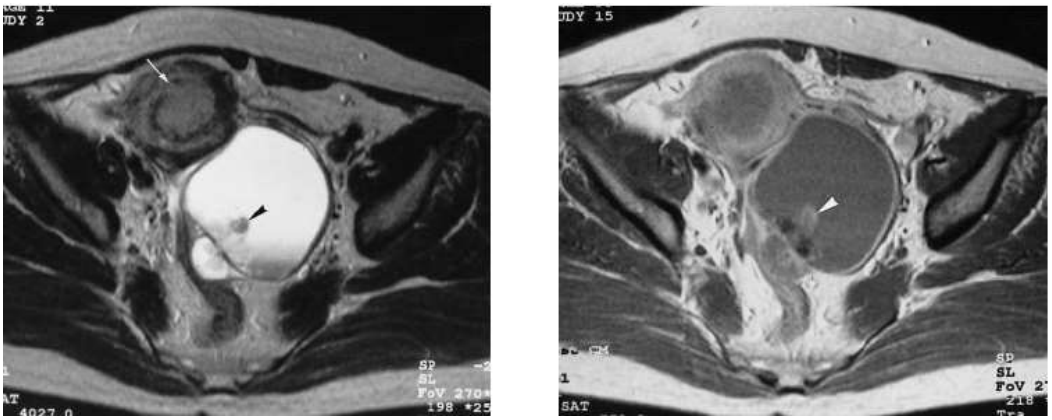

A **B**

Fig. 6: showing endometriod carcinoma with concomitant endometrial carcinoma (a) Axial T2-WI showing a cystic lesion of mixed high and low signal intensity. The solid nodular lesion shows relative low signal intensity (arrow head). Note associated endometrial thickening with disruption of the junctional zone (arrow). (b) Axial post contrast T1 WI showing contrast enhancement in the solid part (arrowhead) **(7).**

Clear cell tumors: appear as unilocular cyst with thick-wall and multiple vascular solid mural nodules. The cyst margin appears smooth. It may be associated with endometriosis or even arise within endometriomas. Its signal on T1 WI varies from low to very high **(8).**

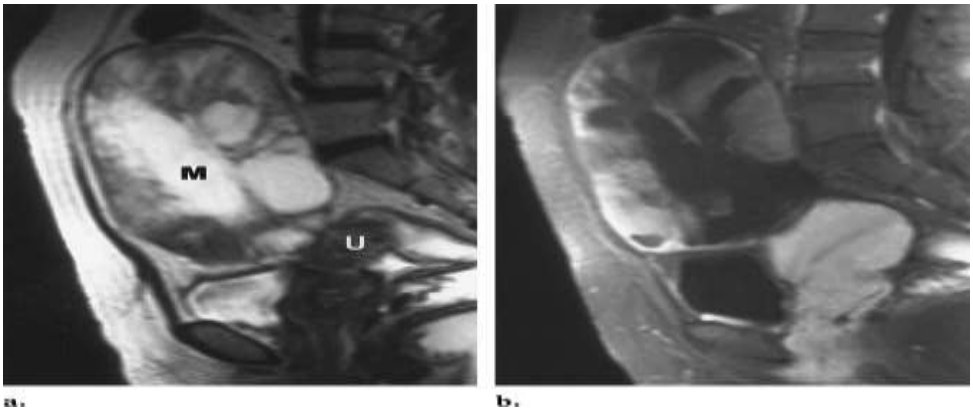

a. b.

Fig. 7: A 42 year old woman with Clear cell carcinoma (a) Sagittal turbo spin-echo T2-WI demonstrates a large cystic mass (M) with hypointense, irregular solid protrusions peripherally. U =uterus. (b) Gd fat-suppressed fast low-angle shot (FLASH) T1-WI demonstrates marked enhancement of the solid portions of the mass **(8).**

Brenner tumors (Transitional cell tumors) appear as a cystic mass which is multilocular with a solid component. Extensive amorphous calcification in the solid components is one characteristic finding of Brenner tumors**,** the solid component usually appears as low signal. On T2 WI As the calcifications are poorly detected by the MRI. **(8).**

Granulose cell tumor: the tumor differs widely in its imaging appearance from being solid tumor with variable degrees of hemorrhagic or fibrotic changes, or cystic lesions that is multilocular to completely cystic tumor**.** The tumor either has intracystic papillary projections or has tendency for peritoneal seeding contrary to epithelial tumors **(5).**

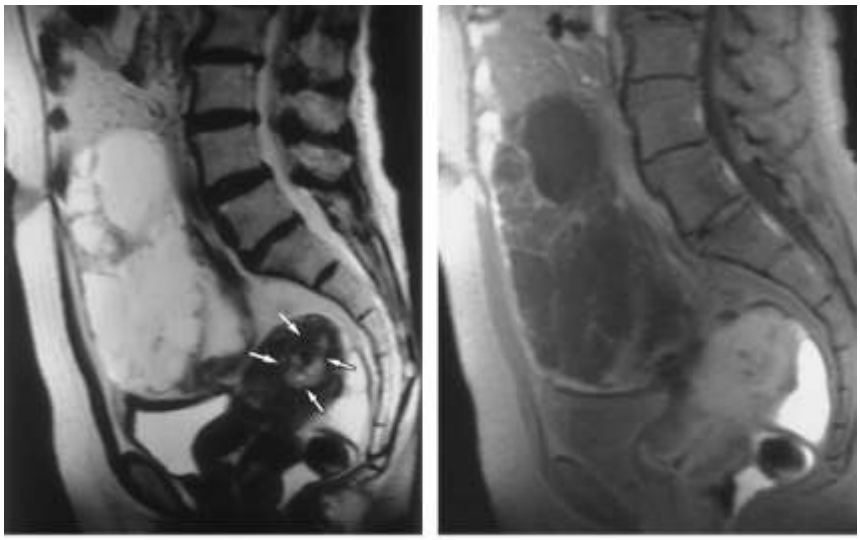

Fig. 8: Granulosa cell tumor in a 71-year-old woman. (a) Sagittal turbo SE T2-WI shows a lobulated multilocular cystic mass. However, no evidence of a papillary projection is noted. The endometrial cavity (arrows) is unusually prominent for a patient this age, a finding that is consistent with endometrial hyperplasia. (b) Gd fat-suppressed FLASH T1-WI demonstrates multiple well-enhanced septae, with numerous large cystic spaces lined by granulosa cells **(8).**

- **Ovarian fibromas and thecomas** they have special imaging criteria owing to its high collagen content that is more or less diagnostic for fibromas.The tumor has low signal intensity On T1-WI. And very low signal intensity On T2-WI, areas of high signal intensity may appear, denoting edema or cystic degeneration. Foci of calcifications also may be seen which are elicited by US or better by CT **(9).**

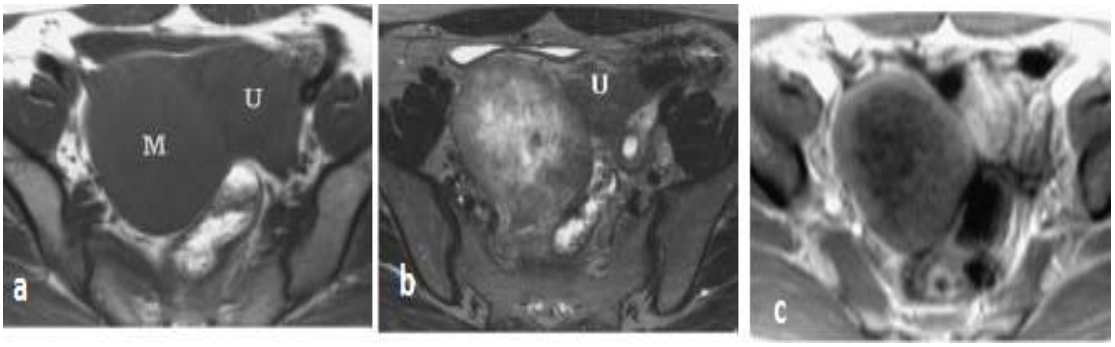

Fig.9: Fibrothecoma in a 46-year-old woman. (a) Axial T1- WI shows a round, low-signal-intensity mass (M) in the right adnexal region. U =uterus. (b) On an axial T2-WI the mass again demonstrates low signal intensity, with central increased signal intensity that represents edema. U =uterus. (c) Gd fat-suppressed T1-WI demonstrates peripheral enhancement of the mass with a central edematous area **(9).**

Sertoli-Leydig Cell Tumor: it is a well-defined solid or sometimes lobulated mass with different-sized intra-tumoral cysts. It shows intermediate signal intensity (which differes according to the fibrous contents of the stroma) On T2-WI and has intense enhancement On T1+ (Gd) **(2).**

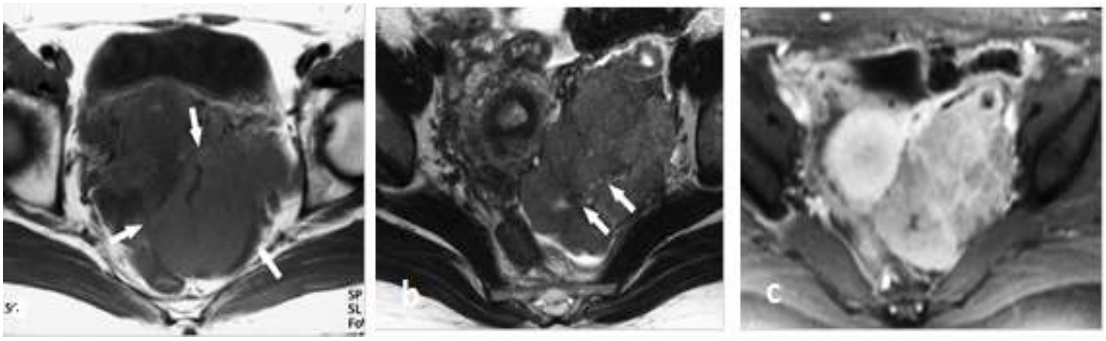

Fig.10: 56-year-old woman with poorly differentiated Sertoli-Leydig cell tumor. A. Axial T1-WI shows lobulated solid mass with low signal intensity (arrows). And B, C. Axial T2-WI shows multi-lobulated mass with intermediate signal intensity with multiple tiny high-signal cysts (arrows). C. Axial post contrast fat suppressed T1-WI shows that mass intensely enhanced **(2).**

Sclerosing stromal tumor is rare benign tumor which happens in young females predominantly causing menstrual abnormalities. The tumor usually obtains large size and is highly vascular. It has high-signal-intensity stroma against low-signal-intensity nodules. On T2 WI and on T1+ (Gd) it is surrounded by a rim of low signal intensity corresponding to compressed ovarian cortex due to a slow growing of the tumor **(10).**

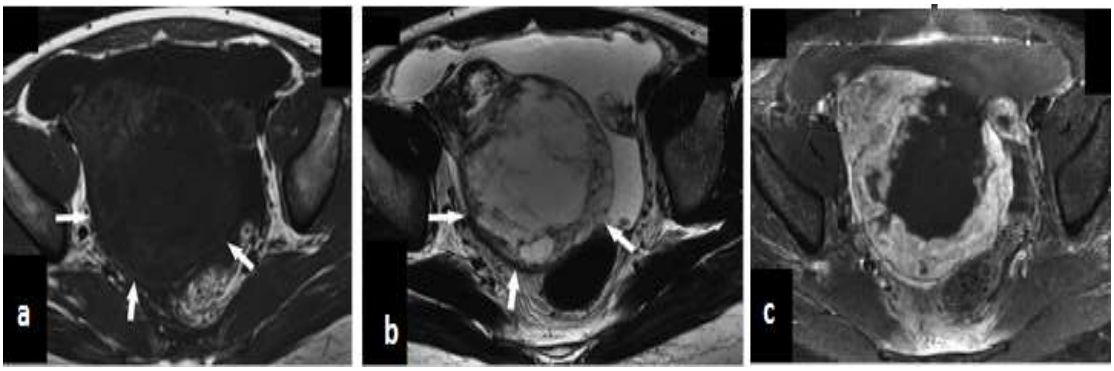

Fig. 11: 34-year-old woman with sclerosing stromal tumor. A, Axial T1-WI shows well-defined pelvic mass with slightly hyperintense peripheral portion (arrows) and irregular central hypointense area. B, Axial T2-WI revealed mass with marked hyperintense central area and slightly hyperintense periphery (arrows). C, Gd fat-suppressed T1-WI reveals very intense enhancement of periphery of tumor **(10).**

Mature cystic teratomas (Dermoid Cysts): They are commonly unilocular, Cystic tumors containing well-differentiated derivatives from at least two of the three germ cell layers "ectoderm, mesoderm, and endoderm" **(5).**It has high signal intensity because of its fat content on T1 WI, variable SI on T2WI. The signal intensity in both T1 and T2 may resemble haemorrhagic lesions mostly endometriomas. Frequency-selective fat suppression technique is helpful for differentiating these two common entities **(10).**

Malignant transformation is supposed if there is transmural invasion of the pelvic organs from a fat containing mass with solid component which is more represented by post contrast assessment **(2).**

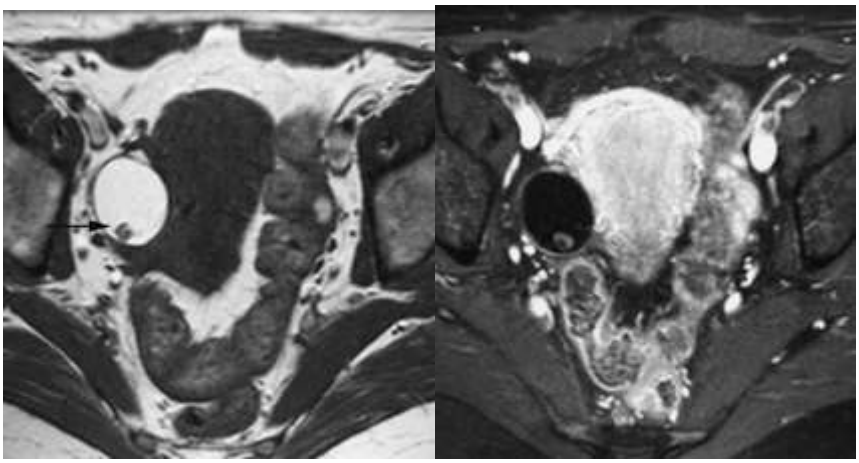

A **B**

Fig. 12 : A 44-year-old woman complaining about irregular menstrual cycle and a suspicious adnexal mass at TVUS (a). Axial T1-WI. The cystic structure of the right ovary demonstrates hyperintense contents with a round nodule in the lower part of the cyst (arrow) (b).Axial T1-WI contrast-enhanced image with fat suppression. Hypointense signal is noted after fat suppression confirming fat nature. At pathology, the round nodule corresponded to a hair ball within a mature cystic teratoma **(11).**

Immature Teratoma: There is no definite diagnostic criteria for immature teratoma, although large, predominantly solid masses with high serum alpha-fetoprotein levels may be associated with a greater possibility. While it is reported that calcifications are scattered in immature teratomas, unlike that in mature teratomas which is localized. **(2).**

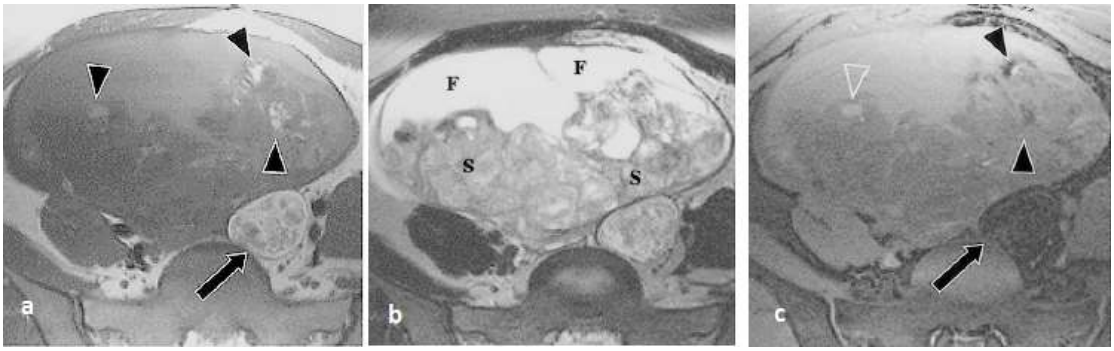

Fig. 13: Immature teratoma associated with ipsilateral mature cystic teratoma in a 27-year-old woman. (a) Axial T1-WI shows a large mass of the left ovary with multiple high signal- intensity foci (arrowheads). A lesion with the typical appearance of a mature cystic teratoma lies adjacent to the mass (arrow). (b) Axial T2-WI shows the large fluid (F) and solid (S) components of the mass. (c) Fat-suppressed T1-weighted FSGE shows that some of the high-signal-intensity foci in a are hemorrhagic and retain their high signal intensity (open arrowhead), whereas others represent foci of fat (solid arrowheads). The ipsilateral mature cystic teratoma demonstrates suppression of the signal of the cyst contents (arrow) **(12).**

- **Dysgerminoma:** Is a rare tumor that affects mainly young women. It is a counterpart to seminoma in males. It appears as multi-lobulated solid masses with prominent fibro-vascular septa **.**On T1-WI it has low signal intensity and intermediate signal with low SI septa and high signal intensity areas of necrosis on T2-WI and on T1+ (Gd) WI: the septa shows strong enhancement **(5).**

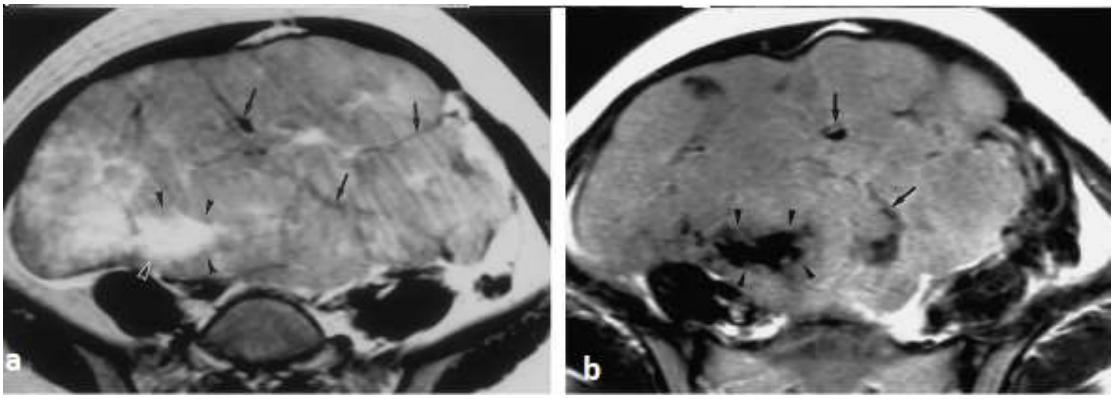

Fig.14: Dysgerminoma in a 17-year-old girl. (a) Axial turbo spin-echo T2-weighted MR image shows a large, multilobulated mass with intermediate signal intensity and persistent low signal intensity of the septa(arrows). The irregular high-signal-intensity areas (arrowheads) indicate necrosis. (b) Axial gadolinium-enhanced turbo spin-echo T1-WI demonstrates relatively homogeneous enhancement with persistent low signal intensity of the septa (arrows) and unenhanced necrotic areas (arrowheads) **(5).**

- **Choriocarcinoma**

Primary ovarian choriocarcinoma either to be gestational or non-gestational in origin. Non-gestational choriocarcinoma has bad prognosis than gestational choriocarcinoma. It appear as a vascular mass with multiple cavities in the solid portion, and areas of necrosis and hemorrhage. High HCG level is a constant finding **(13).**

On ***T1-WI:*** Hemorrhage is seen as hyperintense areas,

On ***T1+(Gd):*** heterogeneous patterns of contrast enhancement have been reported **(5).**Signal voids foci which are seen on both T1- and T2-WI indicate tumor vascularity [127]. The tumor frequently can invade the adjacent organs, thereby demonstrating ill-defined, irregular margins. Pleural effusion, ascites, and lymphadenopathy also have been reported **(2).**

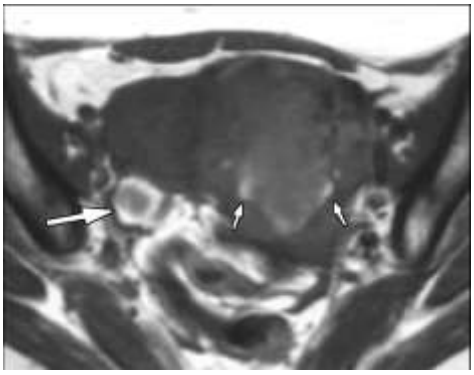

Fig.15: 38-year-old woman who presented with pure primary ovarian choriocarcinoma A, Axial T1-weighted MR image displays hemorrhage in small cavities (small arrows) at periphery of left adnexal mass and right corpus luteum cyst (large arrow) **(13).**

- **Metastasis*:*** Ovarian metastasis account for 10% of all ovarian tumors. They usually occur during the reproductive years. Common sites for ovarian metastasis are the colon and stomach followed by the lung, breast, and contralateral ovary **(15).**Imaging findings usually are nonspecific. It can either present with mainly predominantly solid areas or a combination of cystic and solid areas **(5).**

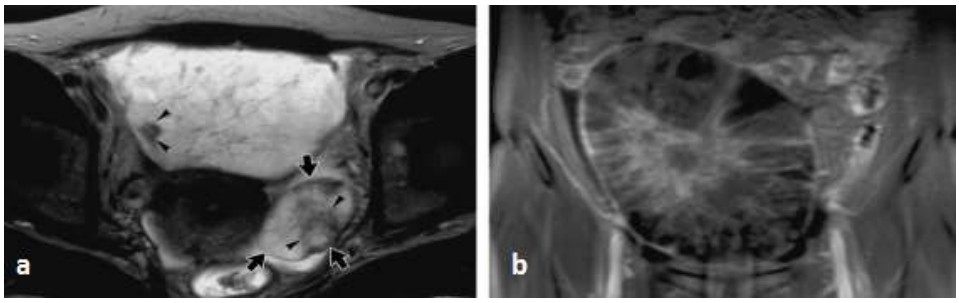

Fig. 16: Bilateral metastasis (Krukenberg tumors) from gastric carcinoma in a 38-year-old woman. (a) Axial T2-WI, shows bilateral cystic masses with hypointense solid portions (arrowheads). The left-sided mass (arrows) is much smaller than the right-sided mass. (b) Gd fat-suppressed T1-WI shows the mass with marked enhancement of the septa and solid components. **(5).**

Krukenberg tumors are metastatic tumors to the ovaries which contain well defined histological characteristics that is mucin secreting "***signet ring***" cells. They usually arise in the GIT**.** They have some characteristic findings on imaging; they appear to be bilateral complex masses. On T1-WI: the solid component has low signal due to the dense stromal reaction, on T2-WI: internal areas of high signal which contain mucin **(5).**

Dynamic Contrast Enhanced MRI (DCE- MRI).

Dynamic enhanced imaging (DCE-MRI) has added to the diagnostic accuracy of these masses, due to its capacity to characterize tumor microcirculation and angiogenesis in malignant tumors. It depends on contrast medium leakage from capillaries into the extravascular extracellular space, therefore enabling quantitative analysis with information on the blood flow as well as vascular permeability **(5).**

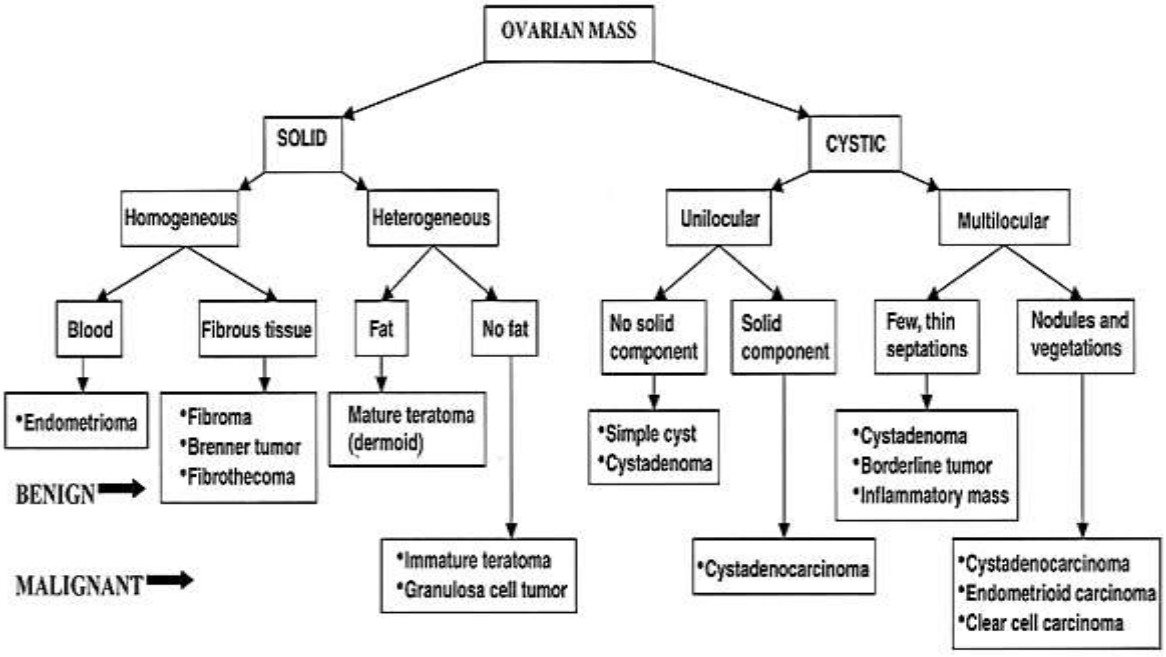

Fig. 17: An algorithm for diagnosis of ovarian mass **(3).**

The signal intensity of the solid components was measured before and then 60 and 120 sec after injection of IV gadolinium, then the percentage of increase in signal intensity is calculated at 60 sec (early) and at 120 sec (late) of enhancement **(14).**

Malignant lesions show greater enhancement than benign lesions during the early phase of enhancement rather than the late phase of enhancement **(14).**

Benign ovarian tumors showed a gradual increase in enhancement without a well-defined peak, while, ***borderline ovarian tumors*** showed moderate initial enhancement followed by a plateau **(15).**

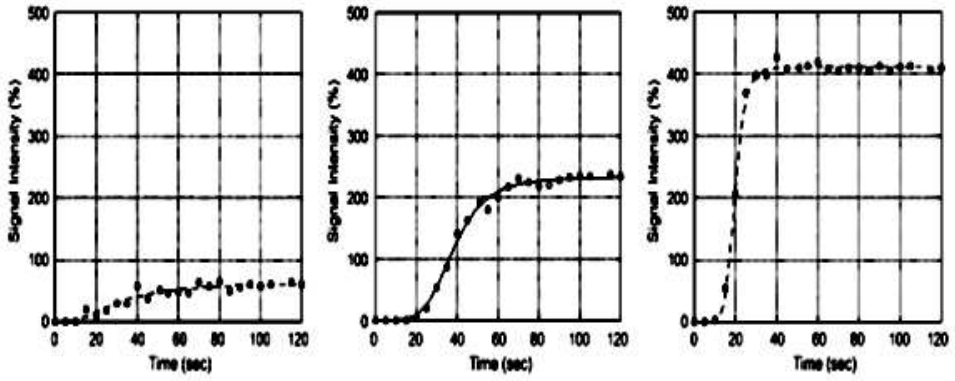

Fig. 18: SI-time curves of (a) benign, (b) borderline, and (c) invasive ovarian tumors. Enhancement curves were fitted to a sigmoid equation. The need for fast dynamic acquisition imposes limitations on the extent of anatomic coverage, which needs to be considered in advanced ovarian cancer. Also the shape, location and heterogeneity of peritoneal deposits can complicate the selection and the operator-dependent definition of regions of interest **(16).**

Combined laboratory and imaging models

The risk of malignancy index (RMI)

The risk of malignancy index (RMI) defined as a simple scoring system depends on menopausal status, ultrasound findings, and serum CA125 level **(16).**

In 1990, the risk of malignancy index (RMI I) was formerly introduced by Jacobs et al **(17).**Afterward, in 1996, a new version of RMI (RMI II) was introduced by Tingulstad et al **(20).** Then modified version of RMI was introduced as RMI III. Finally, in 2009, Yamamoto et al. modified the last present version of RMI, which they have termed: RMI IV **(18).**However, for women with suspected ovarian cancer, the 'RMI I' is the mostly used, widely available, and validated successful triaging system ((**19).**

The available used formula for RMI calculation is:

RMI = *M* ×*US* ×*serum CA-125*.

Where **(M)** refers to the menopausal status of the patient; **(US)** refers to the ultrasound score, and serum **(CA-125)** is the assayed level expressed in U/ml.

RMI 1

For RMI 1, possible abnormal ultrasound findings (U) include multilocular cystic lesion, solid lesion, bilateralism, ascites, and metastasis. If no abnormal finding in the ultrasound report, U is regarded zero (U=0); if a single abnormality is found, it will be U=1; and if two or more abnormal findings are seen, it will be U=2. Menopausal status(M) is either pre-menopausal (M=1) or post-menopausal (more than 1 year after the last menstruation or age > 50 if hysterectomy for any reason) (M=3) or. The serum level of CA125 is entered directly into the formula **(19).**

RMI 2

U is 1 if there are 0–1 abnormal finding and is 4 for 2 or more abnormal findings. M will be 1 for women who are pre-menopausal and 4 in women who are post-menopausal. Again, the serum level of CA125 is entered directly into the formula **(17).**

RMI 3

U=1 for abnormal finding of 0–1 and 3 for abnormal findings of 2 or more. M=1 for pre-menopausal women and 3 for post-menopausal women. Once again, the serum level of CA125 is entered directly into the formula **(20).**

RMI 4

The used formula is U × CA125 × M × S, where U is 1 for 0–1 abnormal finding and 4 for 2 or more abnormal findings. M=1 in pre-menopausal women and 4 for post-menopausal women. The serum level of CA125 is directly entered into the formula. S represents the largest diameter of the mass, which is 1 if <7 cm, and 2 if ≥7 cm, respectively **(18).**

Table (1): Definitions of RMI that were compared in this study (18).

Varieble	Scoring system			
	RMI 1*	RMI 2*	RMI 3*	RMI 4**
Menopausal status (M)				
- Premenopause	1	1	1	1
- Postmenopause	3	4	3	4
Ultrasound score (U)				
- Multilocular				
- Bitaterally	No feature = 0			
- Solid	1 feature = 1	≤ 1 feature = 1	≤ 1 feature = 1	≤ 1 feature = 1
- Ascites	> 1 feature = 3	> 1 feature = 4	> 1 feature = 3	> 1 feature = 4
- Intraabdominal metastasis				
Serum level of CA-125	**Absolute level (U/mL)**			

* Calculation for RMI 1, RMI 2, RMI 3 = M x U x CA-125

** Calculation for RMI 4 = M x U x CA-125 x S (When S = single greatest diameter of tumor size (cm.). If size <7 cm. S = 1, size ≥7 cm. S = 2)

Role of IOTA ADNEX in ovarian tumors:

Recently, the IOTA Group developed the Assessment of Different NEoplasias in the adneXa (ADNEX) model for more detailed characterization of adnexal masses **(21).** The IOTA ADNEX model utilizes a mathematical algorithm with nine predictors to differentiate benign from malignant masses. In addition, the model can differentiate between subtypes of malignant mass. Several centers have validated the performance of the model in their populations. ADNEX predicts the probability that an adnexal tumor is benign, borderline, stage I cancer, stage II-IV cancer, or secondary metastatic cancer (i.e. non-adnexal cancer metastasis to the ovary). Mathematical models were designed for prediction of the four tumour categories: benign, borderline, primary ovarian cancer, and secondary metastatic cancer. The model was created by clinicians and statisticians from the International Ovarian Tumor Analysis (IOTA) group (phase 7 in 2014) and is based on clinical and ultrasound data from about 6000 women collected at 24 centers in 10 countries :Italy, Belgium, Sweden, Czech Republic, Poland, France, UK, China, Spain, and Canada **(21)**

The ADNEX model uses 9 predictors. There are 3 clinical variables, age, serum CA-125 level, and type of center (oncology referral center or other), and 6 ultrasound variables, maximal diameter of lesion, the proportion of solid tissue, more than 10 cyst locules, number of papillary projections, acoustic shadows, and ascites. All patients included needed surgery as determined by the local clinician **(21)**

The reference standard for the ADNEX model was based on histopathological analysis of the excised tissue, and for malignant tumors also on surgical staging using the International Federation of Gynecology and Obstetrics(FIGO)classification. In the database of IOTA, they used 21 histological groups (11 benign and 10 malignant groups) which were reduced to five for the ADNEX model: benign, borderline tumors, stage I invasive, stage II-IV invasive ovarian cancer, and secondary metastatic cancer **(21)**

The use of ADNEX can estimate the risks for a specific patient. As a result, this improves triage and decisions of management, so decreases morbidity and mortality of the adnexal pathology. Of the four groups of malignant tumors, especially the secondary metastases to the ovaries and the borderline malignant ovarian tumors are of particular interest to identify preoperatively **(21)**

How to use IOTA's Soft ADNEX?

Based on multicentric studies, the ADNEX model has been externally validated **(21)**Now, the final ADNEX model is available online and in mobile applications (www.iotagroup.org/adnexmodel/).

After ultrasound examinations, all the measured parameters are introduced in the ADNEX model. The results are obtained. The risk predictions are added for the four malignant subgroups to obtain the total risk of malignancy **(21)**

As an illustrative case, a 59-year-old woman, with the CA125 level was 153 U/ml. On transvaginal ultrasound, a solid ovarian mass was described. The maximal lesion diameter was 59 mm, the maximal diameter of the largest solid component was 59 mm as well, and no acoustic shadowing was showed. There was fluid outside the pouch of Douglas (ascites). When these parameters were introduced in the ADNEX model, the results and column charts were obtained. The risk predictions for the four subgroups were added to obtain the total risk of malignancy, which was 95.3% for this patient. Thus the tumor was likely to be malignant. Then, differentiation between four subgroups was done and observation of predicted risk for secondary metastatic cancer of 21.2% (compared to a baseline risk of 4.0%) and a risk for stage II-IV ovarian cancer of 67.9% (compared to a baseline risk of 14.1%). The predicted risks for the other subgroups are lower (4.6% for stage I cancer and 1.6% for borderline) and are also smaller than the baseline risks **(21)**

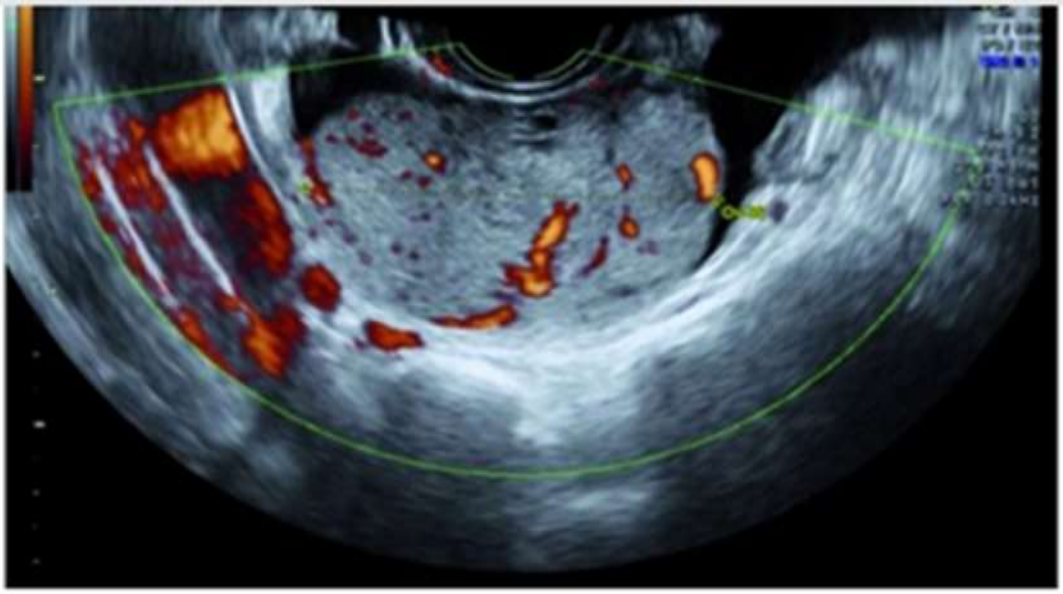

Fig (19)

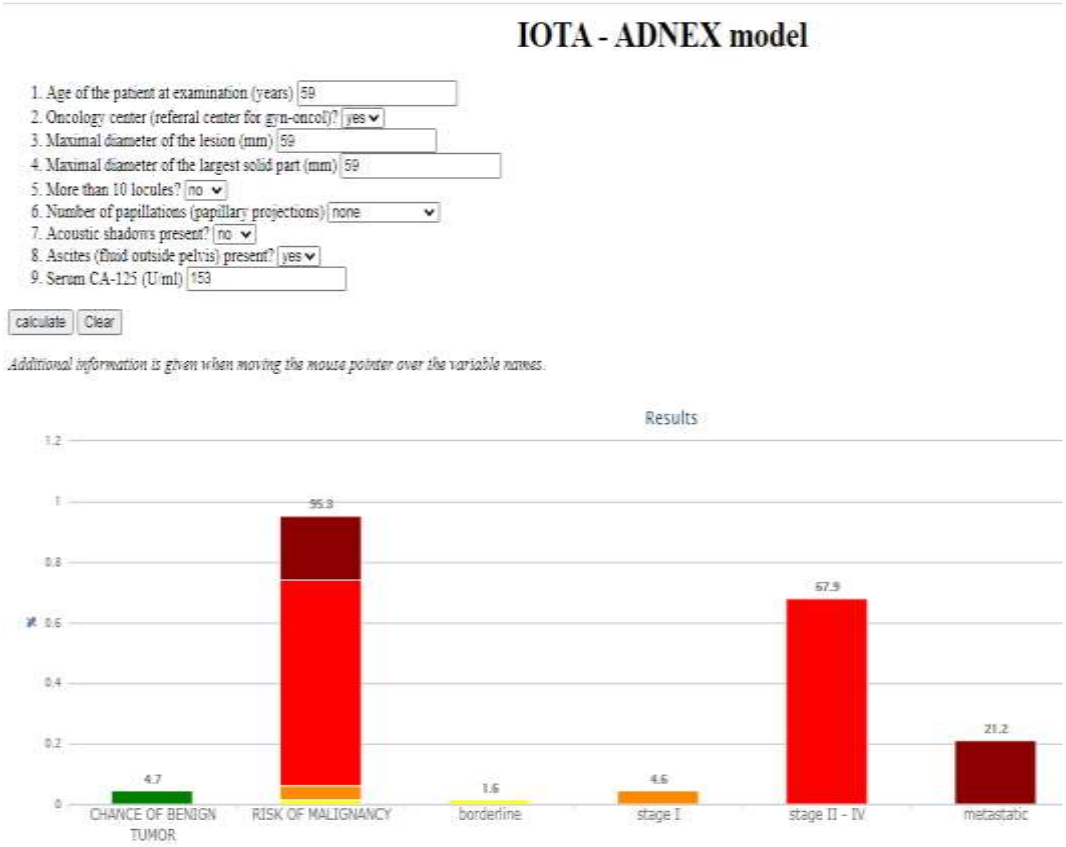

Figure (20): IOTA's Soft Adnex **(21)**

References

1. Iyer VR, Lee SI (2010) MRI, CT, and PET/CT for ovarian cancer detection and adnexal lesion characterization. AJR Am J Roentgenol 194:311–321.
2. Ueno T, Tanaka YO, Nagata M, et al (2004): Spectrum of germ cell tumors: from head to toe. Radiographics Mar-Apr; 24(2): 387-404.
3. Saini A, Dina R, McIndoe G, et al. (2005): Characterization of Adnexal Masses with MRI. AJR March:184 ; 3:1004-1009.
4. Kishimoto K, Ito K, Awaya H, Matsunaga N, Outwater EK, Siegelman ES. (2002): Paraovarian cyst: MR imaging features. Abdom Imaging;27:685– 689.
5. Jung S, Lee J, Rha S, et al. (2002): CT and MR imaging of ovarian tumors with emphasis on differential diagnosis. Radiographics; 22(6): 1305-1325.
6. Jeong YY, Outwater EK, Kang HK(2000): Imaging evaluation of ovarian masses. Radiographics;20:1445-70.
7. Whittaker CS, Coady A, Culver L, Rustin G, Padwick M, Padhani AR (2009) Diffusion-weighted MR imaging of female pelvic tumors: a pictorial review. Radiographics 29:759–774.
8. Matsuoka Y, Ohtomo K, Araki T, et al.(2001): MR imaging of clear cell carcinoma of the ovary. EurRadiol; 11:946–951.
9. Pretorius E, Outwater E, Hunt J, et al. (2001): Magnetic resonance imaging of the ovary. Top MagnReson Imaging; 12:131–146.
10. Kim J, Jung K, Chung D, et al. (2003): Sclerosing stromal tumor of the ovary: MR-pathologic correlation in three cases. Korean J Radiol; 4:194–199.
11. Yamashita Y, Hatanaka Y, Torashima M, et al (1994): Mature cystic teratomas of the ovary without fat in the cystic cavity: MR features in 12 cases. AJR Am J Roentgenol; 163:613–616.
12. Outwater EK, Dunton CJ (1995) Imaging of the ovary and adnexa: clinical issues and applications of MR imaging. Radiology 194:1–18.

13. Bazot M, Darai E, Hourani R, et al. (2004): Deep pelvic endometriosis: MR imaging for diagnosis and prediction of extension of disease. Radiology; 232:379–389.
14. Sohaib A, Sahdev A, Van Trappen P, et al. (2003): Characterization of Adnexal Mass Lesions on MR Imaging . American Journal of Roentgenolog;180: 1297- 1304.
15. Priest AN, Gill AB, Kataoka M, McLean MA, Joubert I, Graves MJ, et al.contrast enhanced MRI in ovarian cancer: initial experience in 3Tesla in Primary and Metastatic Disease Magn Reson Med, 63 (2010), pp. 1044-1049 .
16. Lankester K, Taylor N, Stirling J, et al. (2005): Effects of platinum/taxane based chemotherapy on acute perfusion in human pelvic tumors measured by dynamic MRI. Br. J. Cancer ;93: 979–985.
17. Jacobs IJ, Menon U, Ryan A, Gentry-Maharaj A, Burnell M, Kalsi JK, Amso NN, et al. (2015) Ovarian cancer screening and mortality in the UK Collaborative Trial of Ovarian Cancer Screening (UKCTOCS): a randomised controlled trial. Lancet 387: 945–956.
18. Yamamoto Y, Yamada R, Oguri H, Maeda N, Fukaya T. Comparison of four malignancy risk indices in the preoperative evaluation of patients with pelvic masses. Eur J Obstet Gynecol Reprod Biol 2009; 144(2):163-7
19. Ueland FR, DePriest PD, Pavlik EJ, Kryscio RJ, van Nagell JR, Jr. Preoperative differentiation of malignant from benign ovarian tumors: the efficacy of morphology indexing and Doppler flow sonography. Gynecol Oncol 2003; 91(1):46-50.
20. Tingulstad S, Hagen B, Skjeldestad FE, Onsrud M, Kiserud T, Halvorsen T, et al. Evaluation of a risk of malignancy index based on serum CA125, ultrasound findings and menopausal status in the pre-operative diagnosis of pelvic masses. Br J Obstet Gynaecol 1996; 103(8):826-31.
21. Van Calster B. Presurgical diagnosis of adnexal tumours using mathematical models and scoring systems: a systematic review and meta-analysis. Hum Reprod Update 2014; 20: 449–462.